

Article

Experimental and Simulation Studies for Purification and Etherification of Glycerol from the Biodiesel Industry

Silvia S. O. Silva¹, Matheus R. Nascimento¹ , Ricardo J. P. Lima² , Francisco Murilo Tavares Luna¹ 
and Célio Loureiro Cavalcante Júnior^{1,*} 

¹ Grupo de Pesquisa em Separações por Adsorção, Departamento de Engenharia Química, Universidade Federal do Ceará, Campus do Pici, Bl. 709, Fortaleza 60440-900, CE, Brazil; silviashelly@hotmail.com (S.S.O.S.); matheusrochan@alu.ufc.br (M.R.N.); murilo@gpsa.ufc.br (F.M.T.L.)

² Departamento de Engenharia Mecânica, Universidade Federal do Ceará, Campus do Pici, Bl. 714, Fortaleza 60440-900, CE, Brazil; rjponteslima@icloud.com

* Correspondence: celio@gpsa.ufc.br

Abstract: In this study, a purification route was applied to crude glycerol and its valorization via etherification was evaluated. Crude glycerol samples were obtained through transesterification reactions of soybean oil with methanol using potassium hydroxide as catalyst. A set of separation steps (acidification, neutralization, salt precipitation, evaporation and removal of contaminants using ion-exchange resins) was performed for purification of crude glycerol. The glycerol contents of crude samples were 46% wt., and for purified samples they were above 98% wt. The etherification reactions were carried out with purified samples and different alcohols (ethanol, isopropanol and 3-methyl-1-butanol) placed into a batch reactor, using a small amount of Amberlyst 15 as a catalyst, with autogenous pressure and solvent-free conditions. The glycerol conversion, selectivity and yield to ethers were evaluated. A glycerol conversion of up to 97% wt. was obtained when using ethanol. For isopropanol, the glycerol conversion rate was 85% (97.1% of monoether and 2.8% of diether). However, the selectivity to ethers for 3-methyl-1-butanol was negligible (<3% wt.). A process simulation for the purification and etherification steps integrated with a biodiesel production process was assessed in terms of productivity and energy consumption, considering different scenarios of glycerol/alcohol molar ratios. Finally, main impacts on the overall energy consumption were evaluated for the purification processes (glycerol and ethers).

Keywords: biodiesel; glycerol; purification; etherification



Citation: Silva, S.S.O.; Nascimento, M.R.; Lima, R.J.P.; Luna, F.M.T.; Cavalcante Júnior, C.L. Experimental and Simulation Studies for Purification and Etherification of Glycerol from the Biodiesel Industry. *AppliedChem* **2023**, *3*, 492–508. <https://doi.org/10.3390/appliedchem3040031>

Academic Editor: Jason Love

Received: 3 October 2023

Revised: 27 October 2023

Accepted: 30 October 2023

Published: 3 November 2023



Copyright: © 2023 by the authors. Licensee MDPI, Basel, Switzerland. This article is an open access article distributed under the terms and conditions of the Creative Commons Attribution (CC BY) license (<https://creativecommons.org/licenses/by/4.0/>).

1. Introduction

Transesterification reactions of vegetable oil in the biodiesel industry generate fatty acid methyl (or ethyl) esters and glycerol as products. Theoretically, for every 3 moles of methyl (or ethyl) esters 1 mol of glycerol is obtained, which is equivalent to approximately 10% wt. of the obtained biodiesel. This route has become increasingly relevant due to energy legislation implemented in several countries that promotes the use of biofuels for transportation purposes. Biodiesel fuel demonstrates superiority over diesel, both in terms of human health and impact on the environment, because of its low sulfur content, low particulate emissions and a better CO₂ cycle, thus contributing to global warming reduction [1–4].

The exponential increase in biodiesel production in recent years has generated large-scale growth in the amount of glycerol obtained as a byproduct from the biodiesel industry, consequently generating price reductions in the glycerol market. For this reason, there have been numerous research reports on the use of glycerol to obtain value-added compounds [5–13]. However, the crude glycerol from the biodiesel industry has some impurities that must be treated before using it as a feedstock reagent. Glycerol purification is an important process that is needed to remove impurities (catalysts, salts, residual free fatty acids,

water, mono and diglycerides, etc.). Various studies have been carried out to optimize the purification of crude glycerol. Danish et al. [14] carried out an optimization study of the crude glycerol purification process, using acidification followed by neutralization, solvent extraction and adsorption separation, resulting in an optimal yield of refined glycerol of 83.6%. The purification of glycerol using a combined strategy of physicochemical treatment and membrane filtration, reaching a pure glycerol content of 93.7%, was reported by Chol et al. [15]. Another membrane purification technique, using flat sheets of hydrophobic polyvinylidene fluoride (PVDF) membranes, achieved a pure glycerol content of around 99.9% [16].

Several reaction routes may be performed using glycerol as a reagent, such as the following: acetalization, dehydration, oxidation, esterification and etherification [17–21]. This latter route allows the production of fuel additives, attracting the attention of researchers around the world [22,23]. The glycerol etherification reaction enables its transformation into glycerol ethers, which are compounds that present high stability and applicability. For example, if the etherification reaction is performed with ethanol, which is a short chain alcohol, the reaction products (ethers) may be used both as additives and oxygenated solvents [5,24–28].

Etherification reactions using glycerol generate typical glycerol-based additives. Essentially, the reaction takes place when a glycerol group is protonated in the presence of acid catalysts, with the resulting molecule being ready to “accept” the donor group. Donors may be acetic acid, acetone, acetic anhydride, ethanol and glycerol itself [29]. The reaction of glycerol with ethanol has been increasingly studied lately, since ethanol has a short carbon chain, facilitating the coupling to the glycerol molecule. Monoethylglycerols (MEG), diethylglycerols (DEG) and triethylglycerol (TEG) are the products resulting from the reaction of glycerol with ethanol.

Process simulation is a useful tool for the design, analysis and optimization of biodiesel production processes. Commercially available software such as Aspen Plus, SuperPro Designer, ChemCAD and gPROMS, among others, could be used to design or simulate processes to assess the quantity of feedstocks, products and energy consumption. The DWSIM software is a free alternative that might provide similar performance to commercial ones [30,31]. Analyses and simulations for biodiesel production, techno-economic studies of biorefineries and for energy generation from solid biomass have been performed using DWSIM [32–36].

In this study, the purification of crude glycerol from the processing of biodiesel and its etherification have been evaluated. The purified samples were used to produce ethers using three different alcohols (ethanol, isopropanol and 3-methyl-1-butanol). The reaction conditions were evaluated for glycerol conversion, selectivity and yield for mono-, di- and triethers. Process simulations for the purification and etherification steps were assessed in terms of productivity and energy consumption, considering different scenarios for the etherification reaction.

2. Experimental and Simulation Section

2.1. Materials

The crude glycerol used for purification was obtained from the transesterification reactions of soybean oil (Soya, São Paulo, Brazil), as reported by Canacki and Sanli [37]. Methanol (>99% wt.), ethylene glycol (>99% wt.) and isopropanol (>99% wt.) were purchased from Synth (Diadema, Brazil). Analytical grade reagents (hydrochloric acid and sulfuric acid), amberlite IRA 410 (anionic resin), amberlite IRA 120 (cationic resin) and commercial glycerol (>99% wt.) were purchased from Vetec (Duque de Caxias, Brazil). Potassium hydroxide (85% wt.), activated carbon (97% wt.) and anhydrous sodium periodate (99% wt.) were purchased from Dinâmica (São Paulo, Brazil). Deuterated chloroform (CDCl₃, 99.8%) and Amberlyst 15 were purchased from Sigma-Aldrich (San Luis, USA). 3-Methyl-1-butanol (>99% wt.), hexane (>99% wt.) and ethanol (>99% wt.) were purchased from Neon (Suzano, Brazil).

2.2. Physicochemical and Compositional Characterization

The densities of the crude and purified glycerol were determined according to ASTM D 891-18 [38]. Hydrogenionic potential (pH) was measured using ASTM D1293 [39], with a pH meter from DIGIMED—DM22 (São Paulo, Brazil). The conductivity measurements of the crude and purified glycerol were performed according to ASTM D1125 [40]. The ash content was measured according to the standard method, ISO 2098 [41].

The glycerol content was measured following the sodium periodate method [42], as shown in Equation (1). In this method, glycerol was oxidized with sodium periodate in a strongly acidic medium. The formic acid generated via the reaction was titrated with a standard solution of sodium hydroxide.

$$\text{Glycerol content (\% wt.)} = \frac{9.209 \cdot N \cdot (V_1 - V_2)}{M_i}, \quad (1)$$

where N is the normality of the NaOH solution; V_1 is the volume of NaOH solution spent on the sample (mL); V_2 is the volume of NaOH solution spent on the blank test (mL) and M_i is the mass of crude glycerol or purified glycerol used (g).

The alkalinities of the crude and purified glycerol samples were calculated using Equation (2):

$$\text{Alkalinity (mL} \cdot \text{N/g)} = \frac{100 \cdot V \cdot N}{M_i}, \quad (2)$$

where V is the volume (mL) of the titrant HCl solution for determining the alkalinity of crude, purified and pure glycerol; N is the normality of the HCl solution and M_i is the mass (g) of the glycerol sample used for titration.

Fourier transformed infrared spectroscopy (FTIR) is a technique that was applied to monitor the glycerol purification process and the occurrence of etherification between different alcohols and glycerol. The spectra were measured using a Nicolet™ iS™ 5 FTIR Spectrometer (Thermo Fisher Scientific, Waltham, MA, USA). The samples were scanned in the range of 400–4000 cm^{-1} , with a resolution of 8.0 cm^{-1} . Nuclear magnetic resonance (^1H and ^{13}C) spectra were recorded using a Bruker Avance DRX-500 (Billerica, MA, USA) spectrometer at 500 Hz. The solvent used for the NMR measurements was deuterated chloroform at 25 °C.

Glycerol conversion, selectivity and yield for glycerol mono-, di- and triethers were quantified with gas chromatography (GC), using a Varian 450-GC (Palo Alto, CA, USA) with an autosampler. A capillary column (CP-WAX, 60 m, 0.25 mm diameter and 0.25 mm film thickness) and flame ionization detector (FID) were used for quantification of reagents and products.

The glycerol conversions and selectivities to obtain ethers were calculated using Equations (3) and (4):

$$\text{Conversion (glycerol)} = \frac{C_{g,i} - C_{g,f}}{C_{g,i}}, \quad (3)$$

where $C_{g,i}$ is the initial glycerol concentration (mol/L) and $C_{g,f}$ is the final glycerol concentration (mol/L).

$$\text{Selectivity (ether}(i)) = \frac{C_{ie}}{C_{me} + C_{de} + C_{te}}, \quad (4)$$

where C_{ie} is the concentration of a given ether i (mono-, di- or triether) and C_{me} , C_{de} and C_{te} are the concentrations (mol/L) of monoether, diether and triether, respectively.

2.3. Purification Process for Crude Glycerol

2.3.1. Acidification and Neutralization

The acidification step was performed using a phosphoric acid solution 4M, slowly dropped into 100 g of crude glycerol, with constant stirring, up to pH = 1. This procedure follows a study reported by Nanda et al. [43], which showed that under strongly acidic conditions, almost all alkaline species present in the raw glycerol are neutralized, resulting

in a solid precipitate. The acids then react with the soap to form free fatty acids, leading to better glycerol separation. Subsequently, the samples were transferred to separation funnels to separate the phases.

The acidification performed via the phosphoric acid solution has advantages over other acid solutions, because the phosphate salts have low solubility in the glycerol phase, facilitating their removal. After the acidification step, the glycerol-rich phase was separated using a separation funnel and neutralized to pH 7, using a solution of sodium hydroxide (6 N).

2.3.2. Salt Precipitation and Removal of Contaminants

Following the neutralization step, ethanol was added to the glycerol sample (2:1 ethanol/glycerol mass ratio) and cooled to 0 °C. The cooling process aims to accelerate the precipitation of the salts formed. After 24 h, the precipitated salts were removed via filtration. Activated carbon (2.5 g) was added to the solution to remove impurities. This procedure was performed at 25 °C, with magnetic stirring, for 90 min, and then the activated carbon was removed via filtration.

The removal of ethanol, added for the precipitation of salts, and traces of water from previous steps was performed under vacuum using a Rotavapor (model R-215, Essen, Germany) at 100 °C, 100 rpm for 1 h.

Two ion-exchange commercial resins (Amberlite IRA 120 and IRA 410) were used for removal of anionic and cationic contaminant traces still present in the glycerol samples. The anionic and cationic resins (Amberlite IRA 410 and Amberlite IRA 120, respectively) were activated using a solution of NaOH 4.0% wt. (IRA 410) and a solution of HCl 5.0% wt. (IRA 120) [44]. After the activation, the resins were filtered and then added (2.0 g of cationic resin and 3.0 g of anionic resin) to the glycerol-water solution (50% vol.) for the final purification of the glycerol sample. After that, the resins were separated via filtration and the water was evaporated under vacuum (400 mbar) at 80 °C and 100 rpm for 1 h.

2.4. Experimental Procedures for the Etherification Reaction

The etherification reactions were carried out in a batch reactor (Metalquim, Campinas, Brazil), with autogenous pressure and solvent-free conditions. Preliminary studies were performed to evaluate the performance of small amounts of the catalyst (1 to 3 g) using 20 g of glycerol. In order to define the ideal temperature for the etherification reactions, experiments were carried out between 70 °C and 110 °C, in increments of 10 °C, using a molar ratio of 1:3 glycerol/alcohol, 1.0 g of catalyst and a reaction time of 6 h.

In order to determine the influence of the etherifying agent on this reaction, experiments were conducted using three alcohols: ethanol (C2), isopropanol (C3) and 3-methyl-1-butanol (C5), to assess the conversion of glycerol with increasing size of the alcohol carbon chain. The experimental conditions were varied to evaluate the conversion, selectivity and yield for mono-, di- and triethers. The experiments were performed for both commercial and purified glycerol at the same temperature (110 °C). The parameters were as follows: molar ratio (1:3 to 1:12 for glycerol/alcohol), catalyst load (2.0 g) and reaction time (6 h).

2.5. Purification of Products

Liquid-liquid extraction and distillation were performed to purify the reaction products. Initially, tests were carried out with the objective of assessing the behavior of some solvents (i.e., pentane, hexane and heptane) for the extraction of ethers. After definition of the best solvent (hexane), a mass ratio of reaction mixture to solvent (1:1) was established. Following the liquid-liquid extraction step, the organic phase was distilled at 80 °C for 90 min, under atmospheric pressure using a Kugelrohr apparatus (model B-585, Essen, Germany).

2.6. Process Simulation

DWSIM (Version 8.1.1) is an open-source process simulator, which uses object-based individual models that are resolved in series, representing streams and equipment for an industrial process [31,45]. The DWSIM component library did not contain information on glycerol ethers (mono-, di- and triethers). Therefore, these components were registered according to the UNIFAC methodology. The vegetable oil was represented by triolein. Biodiesel was chosen from the DWSIM component library as methyl oleate. The thermodynamic packages Wilson and NRTL (non-random two-liquid model) were used, considering that both the reactions for obtaining biodiesel and etherification of glycerol take place in liquid. The global process flowsheet, using the DWSIM simulator, is shown in Figure 1.

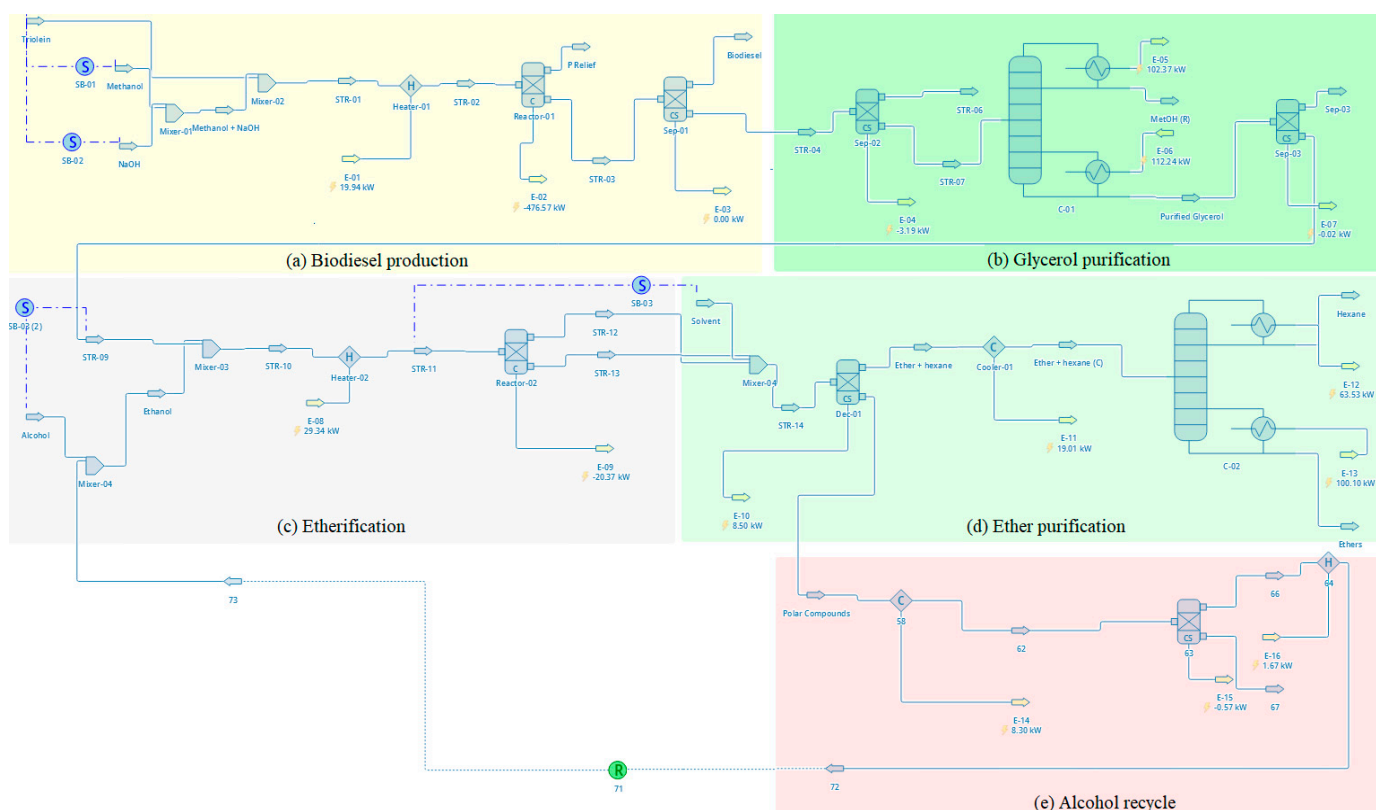


Figure 1. Process flow diagrams of the biodiesel production processes (a), glycerol purification (b), etherification reaction (c), ether purification (d) and alcohol recovery (e).

The simulations for biodiesel production were performed using 1000 kg/h of vegetable oil with a fixed molar ratio of 1:6 (oil/methanol) and catalyst loading (KOH) of 100 g. An isothermal batch reactor was defined for biodiesel production and simulated at 60 °C and a 97% conversion rate. After obtaining biodiesel and glycerol, four steps were carried out to obtain the ethers.

The initial purification of glycerol was simulated with separations using a settler and a distillation column to remove salts, free fatty acids and methanol. After this separation, a glycerol stream with etherifying alcohols (i.e., ethanol and isopropanol) was simulated with three glycerol/alcohol molar ratios: 1:3, 1:6 and 1:12. For the simulation of the etherification reaction a conversion reactor was considered, and the values used were based on the experimental data from this study (temperature = 110 °C, catalyst load = 2.0g and time = 6 h).

After the etherification step, a separation process was used to purify glycerol ethers from crude glycerol, etherifying alcohol and water, simulated using liquid–liquid extraction (with hexane as solvent), a recovery unit for the recycling of etherifying alcohol and a distillation column for recovery of the solvent.

All equipment included in Figure 1 are present in typical industrial plants for traditional biodiesel production. A more efficient use of byproducts and industrial facilities to obtain added-value products tends to increase the profit for a biodiesel manufacturer [7,11,32,33].

3. Results and Discussions

3.1. Physicochemical and Compositional Properties of Purified Glycerol

The physicochemical properties of crude glycerol samples (mean and standard deviation, SD) are shown in Table 1. Typical properties of crude glycerol from the biodiesel industry have been reported in various studies [43,46–49]. Crude glycerol, obtained as a byproduct of the biodiesel processing industry, may have different compositions and properties depending on the raw material, catalyst type and concentration and the transesterification process [43,44]. The crude glycerol produced in the biodiesel industry may also have high methanol content, since excess methanol is normally used in the transesterification reactions, so the glycerol content may vary between 12 and 81% wt.

Table 1. Physicochemical properties of crude glycerol.

Properties	Results (Mean ± SD)	References [43,46–49]
Glycerol content (% wt.)	46.0 ± 0.3	12–81
Alkalinity (mL.N/g)	94.0 ± 0.5	56.0–110.0
Conductivity (µS/cm)	1,894 ± 10	-
Density (g/cm ³) at 20 °C	1.00 ± 0.07	0.9–1.05
Refractive index (at 20 °C)	1.43 ± 0.20	-
pH	10.1 ± 0.5	4.5–10.5
Ash content (% wt.)	3.7 ± 0.2	3.0–6.0

The physicochemical properties of the glycerol samples, before and after the purification steps described before, are shown in Table 2 and compared with the values of the commercial glycerol sample. It can be observed that the glycerol content increased from 46% (Table 1) to 99% wt. (Table 2) after the purification, thus reaching a purity very close to the commercial glycerol sample. Other properties, such as alkalinity and conductivity, were also notably improved after the purification process.

Table 2. Physicochemical properties and composition of the purified and commercial glycerol samples.

Properties	Purified Glycerol (Mean ± SD)	Commercial Glycerol (Mean ± SD)	Methods
Glycerol content (% wt.)	98.99 ± 0.50	99.50 ± 0.40	AOCS EA6-94
Alkalinity (ml.N/g)	0.05 ± 0.02	0.05 ± 0.01	IUPAC/ACD 1980
Conductivity (µS/cm)	0.31 ± 0.06	0.42 ± 0.05	ASTM D1125
Density (g/cm ³) at 20 °C	1.25 ± 0.05	1.26 ± 0.02	ASTM D891
Refractive index (at 20 °C)	1.47 ± 0.20	1.47 ± 0.01	ASTM D1747
pH	7.2 ± 0.5	8.0 ± 0.1	ASTM D1293
Ash content (% wt.)	0.09 ± 0.05	0.06 ± 0.01	ISO 2098

The FTIR spectra of the crude glycerol, commercial glycerol and purified glycerol samples are shown in Figure 2. For the crude glycerol spectrum, a band around 1555 cm⁻¹ was observed, indicating the presence of impurities containing the carboxylate ion (COO⁻), probably from the reaction between a triglyceride and potassium hydroxide. From the spectrum of the purified samples, it may be seen that the aforementioned band was suppressed after the purification. The spectra in the region around 3300 cm⁻¹ show wide and intense bands, due to stretching of the O–H bonds. The area of this band may be

related to the glycerol content in the samples. In fact, more intense bands were observed for the commercial and purified glycerol samples.

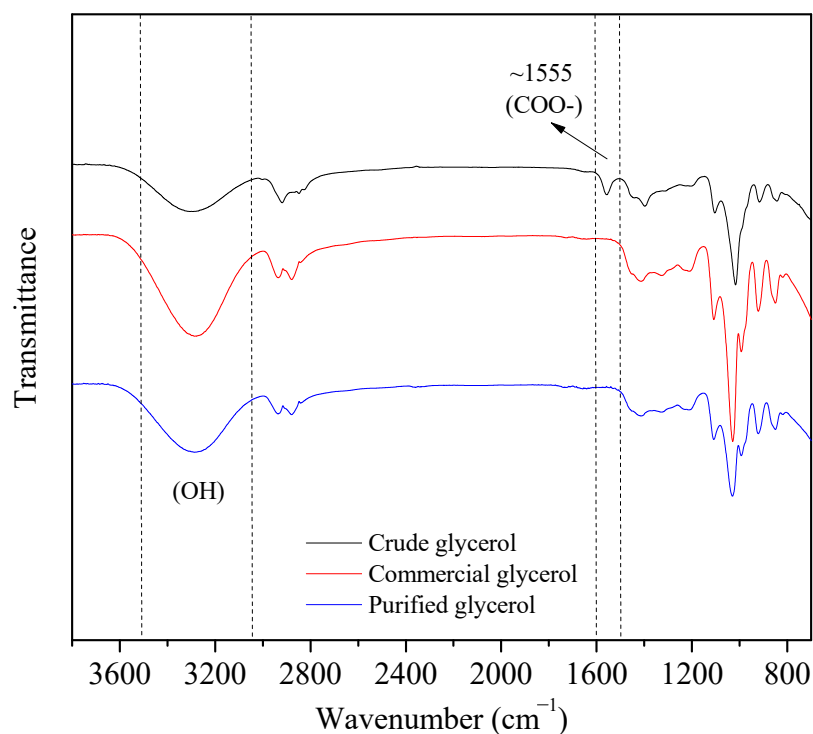


Figure 2. FTIR spectra of crude glycerol (black), commercial glycerol (red) and purified glycerol (blue) samples.

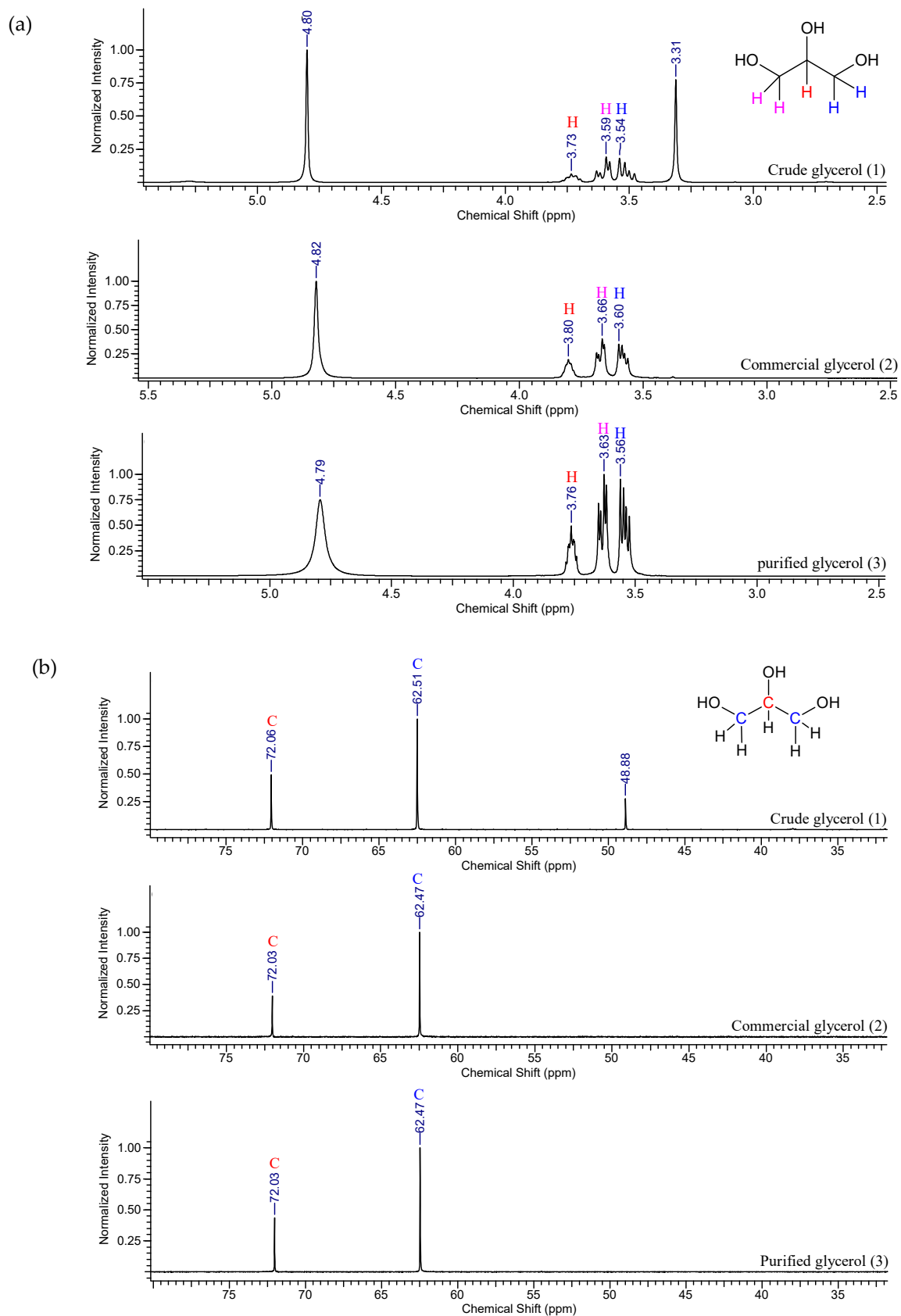
The ^1H and ^{13}C -NMR spectra of the crude, commercial and purified samples are displayed in Figure 3.

The presence of four peaks at 4.82, 3.80, 3.66 and 3.60 ppm can be observed in the ^1H -NMR spectra (Figure 3a), which correspond to hydrogen attached, respectively, to oxygen, to a secondary carbon atom and to the last two primary carbons atoms. The spectrum obtained for the crude glycerol sample shows the same peaks, with a different peak at 3.31 ppm which is probably related to the presence of methoxyl, CH_3O^- , in methyl esters (i.e., residual biodiesel) [48].

For the commercial and purified glycerol samples, the ^{13}C -NMR spectra (Figure 3b) show similar peaks for both samples at 62.47 and 72.03 ppm. These peaks indicate the presence of primary and secondary carbon atoms, respectively, in the molecule. Compared with the spectrum of the crude glycerol sample, in addition to the aforementioned peaks, another one at 48.88 ppm can be observed due to the related impurities from the ester molecules that were saponified during the transesterification reaction. In both NMR spectra of the purified glycerol samples, it is possible to observe that the peaks related to impurities in the crude glycerol sample were suppressed.

3.2. Etherification Reactions

To evaluate the effect of the temperature on the conversion of glycerol, experiments were carried out to obtain the best operating temperature for the etherification reactions using ethanol as the etherifying agent and 1.0 g of Amberlyst 15 as a catalyst (see Figure 4). It may be observed that the glycerol conversion increased with increasing temperature, reaching conversion values above >50% wt. for experiments using temperatures above 60 °C. There is a tendency to increase the glycerol conversion with temperature; however, the experiments were carried out up to 110 °C, because the temperature limitation for the catalyst (Amberlyst 15) is 120 °C.



liquid extractions and distillations were used to remove the solvent thus obtaining a purified reaction product. The experiments were carried out with both commercial and purified glycerol. For the etherification reaction, only purified glycerol was used, as it reached a high degree of purity, the conversions and selectivities to obtain ethers are reported in Table 3. The results are reported only for the C₂ and C₃ alcohols, because the selectivity to ethers for 3-methyl-1-butanol was negligible in the conditions that were studied.

Table 3. Glycerol conversions, selectivities and yields to ethers for different reaction conditions using the purified glycerol sample as a reaction feed with Amberlyst 15® as a catalyst (T = 110 °C and catalyst load = 2.0 g).

Experimental Conditions			Results (% wt.)						
Alcohol	Molar Ratio (Glycerol/Alcohol)	X _G (%)	S _{ME} (%)	η _{ME} (%)	S _{DE} (%)	η _{DE} (%)	S _{TE} (%)	η _{TE} (%)	η _{Total} (%)
Ethanol	1:3	78.3	31.8	24.9	35.3	27.6	32.7	25.6	78.1
Ethanol	1:6	83.4	37.2	31.0	62.7	52.3	0.0	0.0	83.3
Ethanol	1:12	97.5	19.5	19.0	37.6	36.7	42.8	41.7	97.4
Isopropanol	1:3	56.0	97.1	54.4	2.8	1.6	0.2	0.1	56.1
Isopropanol	1:6	79.8	97.6	77.9	2.4	1.9	0.0	0.0	79.8
Isopropanol	1:12	85.2	97.1	82.7	2.8	2.4	0.0	0.0	85.1

X_G is the glycerol conversion; S is the selectivity to ethers; η is the yield to ethers; subscripts ME, DE, TE and Total refer to monoethers, diethers, triethers and total ethers, respectively.

It can be seen in Table 3 that the highest conversion values were obtained for the conditions of higher catalyst loads, alcohol/glycerol ratio and reaction time, as expected. However, a reduction in the yield to ethers was observed using the higher conversion conditions; this may be explained by the increased availability of molecules in the reaction medium that are more favorable to the formation of side products. The selectivities to obtain triethers were negligible when using isopropanol (<1.0% wt.).

3.3. Chemical Characterization of the Etherification Products

The FTIR spectra of the samples obtained using C₂ and C₃ alcohols as etherifying agents are presented in Figure 6. The formation of ether occurs when the hydrogen in the hydroxyl group is replaced with an alkyl group that causes a change in the corresponding ether spectrum. The ether groups were evidenced for all purified samples (ES1—ethers from ethanol and ES2—ethers from isopropanol). The appearance of bands around 1070–1150 cm⁻¹ indicates the presence of aliphatic ethers (C-O-C). The bands in the region between 2800 and 2900 cm⁻¹, which corresponds to C-H aliphatic vibrations, were slightly different due the amount of mono-, di- and triethers existing in the ES1 and ES2 samples. At around 3300 cm⁻¹, the bands are due to the stretching of O-H bonds. For ether samples using isopropanol (ES2), a band near 1720 cm⁻¹, associated to the carbonyl group (C=O), may be due to the formation of side products, probably related to the presence of hydroxy acetone, eventually generated from the dehydration of the glycerol molecule [18]. This band was not observed for the sample obtained for the reaction using ethanol as the etherifying agent.

The ¹³C-NMR spectra of the products obtained from the reactions using ethanol and isopropanol are shown in Figure 7. There are five peaks, relative to carbons present in the ethers. The formation of triethers was not identified in the ¹³C-NMR spectra, due to very low concentration of triethers in the samples, as already previously observed in the chromatographic results (see Table 3).

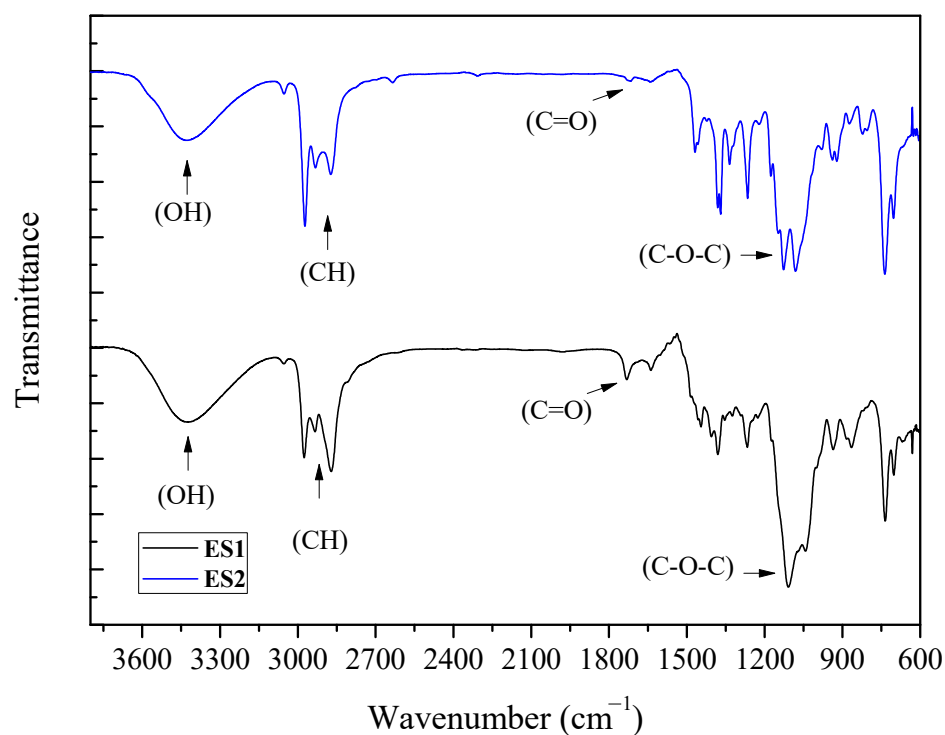


Figure 6. FTIR spectra of the samples obtained for the etherification reactions: glycerol/alcohol molar ratio of 1:3, temperature of 110 °C, 1.0 g of catalyst and reaction time of 6 h. Etherifying alcohols: ethanol (ES1) and isopropanol (ES2).

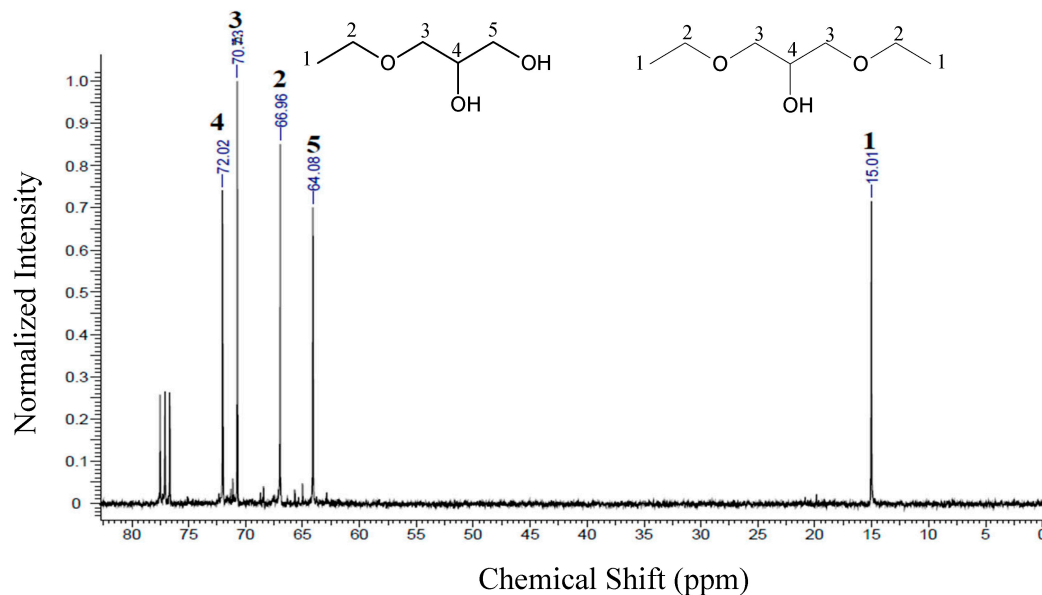


Figure 7. ^{13}C -NMR of the samples obtained for the etherification reactions, using ethanol (ES1). Conditions: glycerol/alcohol molar ratio of 1:3, temperature of 110 °C, 1.0 g of catalyst and reaction time of 6h.

For ether samples obtained using ethanol (ES1), the chemical shifts presented for carbons 1, 2, 3 and 4 were the same for the two molecules (monoethylglycerols and diethylglycerols). For the monoethylglycerols, a peak at 64.08 ppm was observed corresponding to the presence of carbon 5. For ether samples using isopropanol (ES2, see Figure 8) there is no significant formation of trisubstituted ethers; since these compounds would present high steric hindrance, their formation becomes much more difficult [49]. Accordingly, the

peaks observed in Figure 8 for ES2 mainly indicate the formation of mono- and diether molecules (3-isopropoxy-1,2-propanediol and 1,3-diisopropoxy-2-propanol).

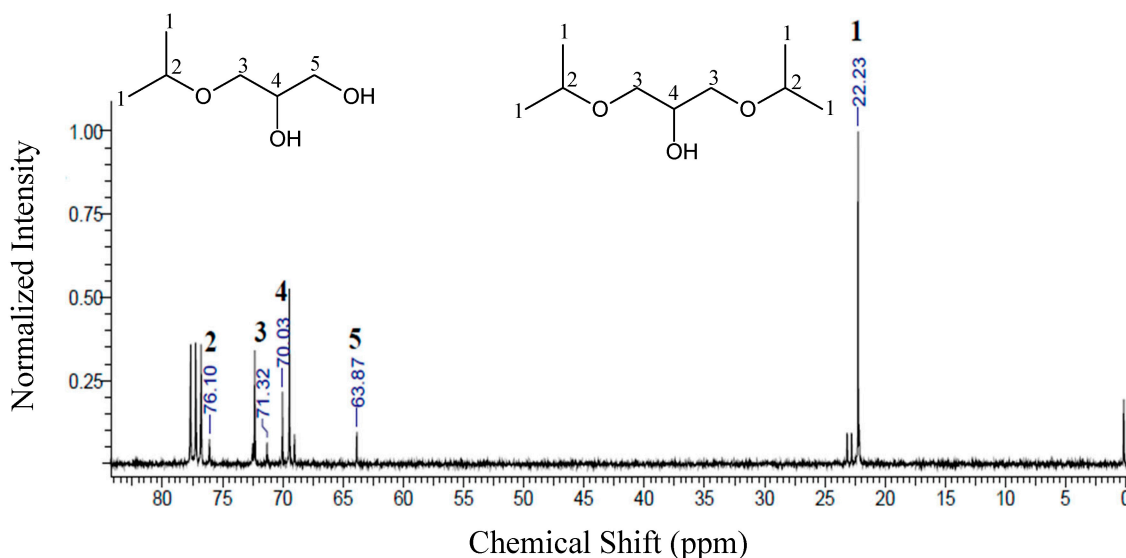


Figure 8. ^{13}C -NMR of the samples obtained for the etherification reactions, using isopropanol (ES2). Conditions: glycerol/alcohol molar ratio of 1:3, temperature of 110 °C, 1.0 g of catalyst and reaction time of 6 h.

3.4. Process Simulation Using DWSIM

A flexible industrial system capable of producing both biodiesel and glycerol ethers was simulated using DWSIM. All equipment included in the simulation is present in a typical industrial plant for biodiesel production. The results for the simulation of the glycerol purification process are shown in Table 4. The material balance data for the biodiesel production and the solvent recovery are shown in Table S1 and Table S2, respectively. Due to the negligible selectivity to ethers when using 3-methyl-1-butanol, the simulations were performed only using ethanol and isopropanol, at three glycerol/alcohol molar ratios: 1:3, 1:6 and 1:12.

Table 4. Simulation results for process of glycerol purification.

Conditions	Input		Output	
	STR-04	STR-06	Methanol	Glycerol
Temperature (°C)	60.0	60.0	64.8	45.3
Pressure (bar)	1.01	1.01	1.01	1.01
Mass Flow (kg/h)	222.81	10.00	116.97	840.63
Volumetric Flow (m ³ /h)	0.26	0.00	0.16	1.07
Specific Enthalpy (kJ/kg)	−936.31	570.49	−1041.42	−722.99
Component mole fraction	STR-04	STR-06	Methanol	Glycerol
Methanol	0.729	0.000	0.990	0.000
Catalysts and salts	0.052	1.000	0.000	0.000
Glycerol	0.219	0.000	0.010	1.000

STR-04: Crude glycerol from biodiesel production; STR-06: catalysts and salts stream.

The glycerol purification flowsheet is shown in Figure 1b. The crude glycerol from biodiesel processing was constituted by 21.9% of glycerol, 72.9% of methanol and 5.2% of catalysts, salts and other impurities. The set consisted of two separators for removing catalysts and salts and a distillation column for methanol separation. In Table 4, the outlet

compositions of the main streams and the high specific enthalpy (-1041.42 kJ/kg) for methanol separation are shown.

The set for the etherification process was simulated using two mixers, a heater and a conversion reactor (see Figure 1c). The input and output data for the etherification process with a 1:3 glycerol/ethanol molar ratio at 110 °C are presented in Table 5. In this simulation, unreacted ethanol (16.0% mol) in the liquid phase is recovered in the ether purification process (Figure 1d) and alcohol recycle unit (Figure 1e). The simulation results for the etherification process using glycerol/isopropanol with a molar ratio of 1:3 are reported in Table 6. It may be observed that changing the alcohol (C_2 to C_3) in the etherification reaction increases the amount of ethers in the liquid phase (32% to 50.5% mol). However, the mass flow of isopropanol in the vapor phase (STR-12) also increases due to unreacted alcohol in the system. The simulation for the etherification process is important to estimate the productivity of ethers and the global energy consumption for the overall glycerol valorization process. The process optimization should identify the best operational conditions for further viability assessment.

Table 5. Simulation results for the etherification reaction using glycerol/ethanol with a molar ratio of 1:3 at 110 °C.

Etherification with Ethanol (1:3 Molar Ratio)				
Conditions	Input		Output	
	Glycerol	Ethanol	STR-12	STR-13
Temperature (°C)	229.2	25.0	110.0	110.0
Pressure (bar)	1.01	1.01	1.01	1.01
Mass Flow (kg/h)	95.51	143.32	59.62	179.21
Volumetric Flow (m ³ /h)	0.09	0.18	51.91	0.20
Spec. Enthalpy (kJ/kg)	-477.09	-922.33	137.42	-614.17
Component mole fraction				
Ethanol	0.000	1.000	0.636	0.160
Glycerol	1.000	0.000	0.000	0.091
3-ethoxypropan-1,2-diol	0.000	0.000	0.000	0.095
1,3-diethoxypropan-2-ol	0.000	0.000	0.000	0.114
1,2,3-triethoxypropane	0.000	0.000	0.000	0.112
Water	0.000	0.000	0.361	0.425

STR-12: reaction mixture (vapor phase) and STR-13: reaction mixture (liquid phase).

Table 6. Simulation results for the etherification reaction using glycerol/isopropanol with a molar ratio of 1:3 at 110 °C.

Etherification with Isopropanol (1:3 Molar Ratio)				
Conditions	Input		Output	
	Glycerol	Isoprop.	STR-12	STR-13
Temperature (°C)	229.2	25.0	110.0	110.0
Pressure (bar)	1.01	1.01	1.01	1.01
Mass Flow (kg/h)	95.51	745.13	675.91	164.72
Volumetric Flow (m ³ /h)	0.09	0.95	371.02	0.19
Spec. Enthalpy (kJ/kg)	-477.09	-754.49	140.44	-587.04
Component mole fraction				
Isopropanol	0.000	1.000	0.932	0.335
Glycerol	1.000	0.000	0.000	0.127
3-ethoxypropan-1,2-diol	0.000	0.000	0.000	0.494
1,3-diethoxypropan-2-ol	0.000	0.000	0.000	0.011
Water	0.000	0.000	0.067	0.031

STR-12: reaction mixture (vapor phase) and STR-13: reaction mixture (liquid phase).

The input and output data for the simulation of the etherification process with a 1:6 and 1:12 glycerol/alcohol molar ratio are reported in Table S3 and Table S4. It may be noted that increasing the molar ratio in the etherification reaction increases the productivity of ethers (from 116.1 to 119.2 kg/h, when using C₂ alcohol and from 73.9 to 97.8 kg/h, when using C₃ alcohol); however, the energy for recovery of the alcohol excess rises considerably. The simulation results for ether purification are reported in Table S5.

The specific energy consumption, in MJ/kg of product, is a basic approach to estimate the energy needs for a given process. The energy consumption estimates, for different molar ratios evaluated in the etherification reactions, are compared in Figure 9, considering the energy demands of all equipment in the biodiesel production plant. It may be noted that the estimated specific energy consumption was considerably lower for processes using C₂ instead of C₃ alcohol. This fact was related mainly to the energy demands for the ether purification and alcohol recovery units.

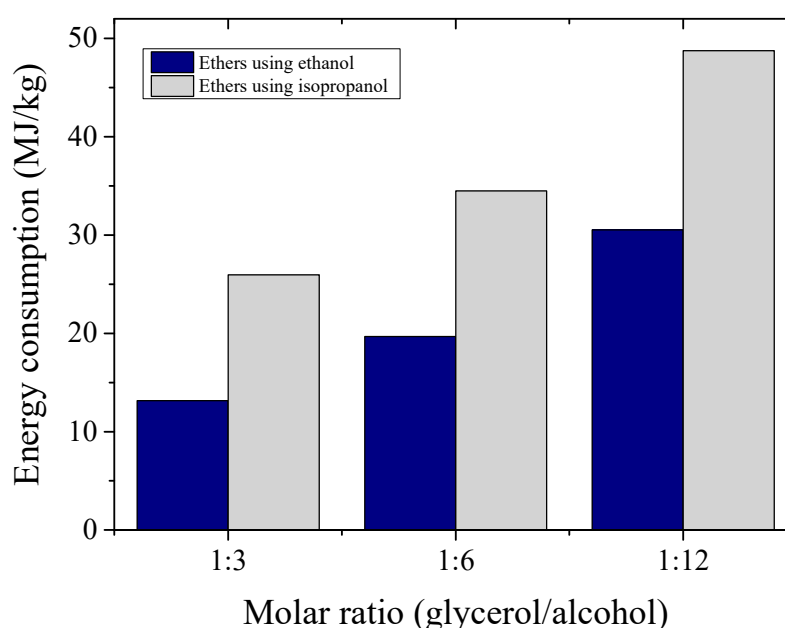


Figure 9. Simulation of specific energy consumptions for the production of glycerol ethers using ethanol and isopropanol at different molar ratios.

4. Conclusions

The valorization of glycerol, using chemical routes that could be operated in the current existing biodiesel industrial plants, was evaluated in this study, starting with the purification of crude glycerol. The glycerol contents of purified samples were above 98%. The physicochemical properties of the glycerol samples after the purification steps were similar to those of commercial glycerol samples.

The etherification reactions of glycerol at the laboratory scale, using Amberlyst 15 and C₂ and C₃ alcohols, presented conversion values up to 97%. The results of the etherification reaction of purified glycerol were very promising for both C₂ and C₃ alcohols. Low selectivity to ethers was observed when using C₅ alcohol (<3% wt.).

The influences of temperature, glycerol/alcohol molar ratio, catalyst load and reaction time were evaluated. Conversion values above 90% wt. were obtained when using C₂ alcohol, with excellent yield of ethers (up to 97.4%). Also, with C₃ alcohol as the etherifying agent, glycerol conversions reached up to 85% with calculated selectivities of 97.1% and 2.8%, for monoether and diether, respectively.

An industrial system capable of producing both biodiesel and glycerol ethers was simulated using DWSIM. The productivity of ethers and the global energy consumption for glycerol valorization were estimated. The results obtained in this study show that valorization of crude glycerol, using chemical routes that could be operated within existing

biodiesel industry facilities, could be achieved to obtain chemicals that could be used as value-added fuel additives. In addition, strategies of optimization for energy consumption, such as energetic integration, would be relevant to reduce costs and to increase the process viability.

Supplementary Materials: The following supporting information can be downloaded at: <https://www.mdpi.com/article/10.3390/appliedchem3040031/s1>, Table S1: Input and output data for the process of biodiesel production; Table S2: Input and output data for the alcohol recycle unit; Table S3: Input and output data for the etherification reaction using ethanol and isopropanol at 110 °C and a molar ratio of 1:6 (glycerol/alcohol); Table S4: Input and output data from DWSIM for the etherification reaction using ethanol and isopropanol at 110 °C and a molar ratio of 1:12 (glycerol/alcohol); Table S5: Input and output data for the ether purification process (etherification using a glycerol/ethanol molar ratio of 1:3 at 110 °C); Table S6: Input and output data for the ether purification process (etherification using a glycerol/isopropanol molar ratio of 1:3 at 110 °C).

Author Contributions: S.S.O.S.: conceptualization, methodology, formal analysis, investigation and writing—original draft preparation; M.R.N.: methodology, software and validation; R.J.P.L.: conceptualization, investigation and writing—original draft preparation; F.M.T.L.: methodology, formal analysis, software, resources, writing—review and editing and supervision; C.L.C.J.: resources, writing—review and editing and supervision. All authors have read and agreed to the published version of the manuscript.

Funding: This research was funded by Coordenação de Aperfeiçoamento de Pessoal de Nível Superior (CAPES), Conselho Nacional de Desenvolvimento Científico e Tecnológico (CNPq) and Fundação Cearense de Apoio ao Desenvolvimento Científico e Tecnológico (FUNCAP).

Institutional Review Board Statement: Not applicable.

Informed Consent Statement: Not applicable.

Data Availability Statement: The data presented in this study are available in the article and the Supplementary Materials.

Conflicts of Interest: The authors declare no conflict of interest.

References

1. Pramanik, T.; Tripathi, S. Biodiesel: Clean fuel of the future: New processing technologies uncover means to produce low-sulfur biomass-based diesel. *Hydrocarb. Process.* **2005**, *84*, 49–54.
2. Knothe, G.; Van Gerpen, J.; Krahl, J. *The Biodiesel Handbook*; Elsevier: Champaign, IL, USA, 2005.
3. Bournay, L.; Casanave, D.; Delfort, B.; Hillion, G.; Chodorge, J.A. New heterogeneous process for biodiesel production: A way to improve the quality and the value of the crude glycerin produced by biodiesel plants. *Catal. Today* **2005**, *106*, 190–192. [[CrossRef](#)]
4. Bueno, A.V.; Pereira, M.P.; Pontes, J.V.O.; Luna, F.M.; Cavalcante, C.L., Jr. Performance and emissions characteristics of castor oil biodiesel fuel blends. *Appl. Therm. Eng.* **2017**, *125*, 559–566. [[CrossRef](#)]
5. Melero, J.A.; Vicente, G.; Paniagua, M.; Morales, G.; Muñoz, P. Etherification of biodiesel-derived glycerol with ethanol for fuel formulation over sulfonic modified catalysts. *Bioresour. Technol.* **2012**, *103*, 142–151. [[CrossRef](#)]
6. Monteiro, M.R.; Kugelmeier, C.L.; Pinheiro, R.S.; Batalha, M.O.; da Silva César, A. Glycerol from biodiesel production: Technological paths for sustainability. *Renew. Sust. Energ. Rev.* **2018**, *88*, 109–122. [[CrossRef](#)]
7. Rodrigues, A.; Bordado, J.C.; Santos, R.G. Upgrading the glycerol from biodiesel production as a source of energy carriers and chemicals—A technological review for three chemical pathways. *Energies* **2017**, *10*, 1817. [[CrossRef](#)]
8. Veluturla, S.; Archana, N.; Subba Rao, D.; Hezil, N.; Indrajya, I.S.; Spoorthi, S. Catalytic valorization of raw glycerol derived from biodiesel: A review. *Biofuels* **2016**, *9*, 305–314. [[CrossRef](#)]
9. Bagheri, S.; Julkapli, N.M.; Yehye, W.A. Catalytic conversion of biodiesel derived raw glycerol to value added products. *Renew. Sustain. Energy Rev.* **2015**, *41*, 113–127. [[CrossRef](#)]
10. Tan, H.W.; Abdul Aziz, A.R.; Aroua, M.K. Glycerol production and its applications as a raw material: A review. *Renew. Sustain. Energy Rev.* **2013**, *27*, 118–127. [[CrossRef](#)]
11. Quispe, C.A.G.; Coronado, C.J.R.; Carvalho, J.A., Jr. Glycerol: Production, consumption, prices, characterization and new trends in combustion. *Renew. Sustain. Energy Rev.* **2013**, *27*, 475–493. [[CrossRef](#)]
12. Anuar, M.R.; Abdullah, A.Z. Challenges in biodiesel industry with regards to feedstock, environmental, social and sustainability issues: A critical review. *Renew. Sustain. Energy Rev.* **2016**, *58*, 208–223. [[CrossRef](#)]
13. Mehrpooya, M.; Ghorbani, B.; Abedi, H. Biodiesel production integrated with glycerol steam reforming process, solid oxide fuel cell (SOFC) power plant. *Energ. Convers. Manag.* **2020**, *206*, 112467. [[CrossRef](#)]

14. Danish, M.; Mumtaz, M.W.; Fakhar, M.; Rashid, U. Response surface methodology based optimized purification of the residual glycerol from biodiesel production process. *Chiang Mai J. Sci.* **2017**, *44*, 1570–1582.
15. Chol, C.G.; Dhabhai, R.; Dalai, A.K.; Reaney, M. Purification of crude glycerol derived from biodiesel production process: Experimental studies and techno-economic analyses. *Fuel Process. Technol.* **2018**, *178*, 78–87. [CrossRef]
16. Pal, P.; Chaurasia, S.P.; Upadhyaya, S.; Agarwal, M.; Sridhar, S. Glycerol purification using membrane technology. In *Membrane Processes: Pervaporation, Vapor Permeation and Membrane Distillation for Industrial Scale Separations*; Scrivener Publishing LLC: Beverly, MA, USA, 2018; pp. 431–463. [CrossRef]
17. Poly, S.S.; Jamil, M.A.; Touchy, A.S.; Yasumura, S.; Siddiki, S.H.; Toyao, T.; Maeno, Z.; Shimizu, K.I. Acetalization of glycerol with ketones and aldehydes catalyzed by high silica H β zeolite. *Mol. Catal.* **2019**, *479*, 110608. [CrossRef]
18. Mazarío, J.; Concepción, P.; Ventura, M.; Domine, M.E. Continuous catalytic process for the selective dehydration of glycerol over Cu-based mixed oxide. *J. Catal.* **2020**, *385*, 160–175. [CrossRef]
19. Arcanjo, M.R.A.; Silva, I.J.; Rodríguez-Castellón, E.; Infantes-Molina, A.; Vieira, R.S. Conversion of glycerol into lactic acid using Pd or Pt supported on carbon as catalyst. *Catal. Today* **2017**, *279*, 317–326. [CrossRef]
20. Jiang, Y.; Li, X.; Zhao, H.; Hou, Z. Esterification of glycerol with acetic acid over SO₃H—functionalized phenolic resin. *Fuel* **2019**, *255*, 111542. [CrossRef]
21. Lemos, C.O.T.; Rade, L.L.; Barrozo, M.A.S.; Cardozo-Filho, L.; Hori, C.E. Study of glycerol etherification with ethanol in fixed bed reactor under high pressure. *Fuel Process. Technol.* **2018**, *178*, 1–6. [CrossRef]
22. Izquierdo, J.F.; Montiel, M.; Palés, I.; Outon, P.R.; Galán, M.; Jutglar, L.; Villarrubia, M.; Izquierdo, M.P.; Hermo, M.P.; Ariza, X. Fuel additives from glycerol etherification with light olefins: State of the art. *Renew. Sustain. Energy Rev.* **2012**, *16*, 6717–6724. [CrossRef]
23. Bozkurt, Ö.D.; Tunç, F.M.; Bağlar Çelebi, N.S.; Günbaş, İ.D.; Uzun, A. Alternative fuel additives from glycerol by etherification with isobutene: Structure–performance relationships in solid catalysts. *Fuel Process. Technol.* **2015**, *138*, 780–804. [CrossRef]
24. Pariente, S.; Tanchoux, N.; Fajula, F. Etherification of glycerol with ethanol over solid acid catalyst. *Green Chem.* **2009**, *11*, 1256–1261. [CrossRef]
25. Yuan, Z.; Xia, S.; Chen, P.; Hou, Z.; Zheng, X. Etherification of biodiesel-based glycerol with bioethanol over tungstophosphoric acid to synthesize glyceryl ethers. *Energ. Fuel* **2011**, *25*, 3186–3191. [CrossRef]
26. Pinto, B.P.; Lyra, J.T.; Nascimento, J.A.C.; Mota, C.J.A. Ethers of glycerol and ethanol as bioadditives for biodiesel. *Fuel* **2016**, *168*, 76–80. [CrossRef]
27. Mravec, D.; Turan, A.; Filková, A.; Mikesková, N.; Volkovicsová, E.; Onyestyák, G.; Harnos, S.; Lóny, F.; Valyon, J.; Kaszonyi, A. Catalytic etherification of bioglycerol with bioethanol over H-Beta, H-Y and H-MOR zeolites. *Fuel Process. Technol.* **2017**, *159*, 111–117. [CrossRef]
28. Veiga, P.M.; Gomes, A.C.L.; Veloso, C.O.; Henriques, C.A. Acid zeolites for glycerol etherification with ethyl alcohol: Catalytic activity and catalyst properties. *Appl. Catal. A-Gen.* **2017**, *548*, 2–15. [CrossRef]
29. Pinzi, S.; Garcia, I.L.; Lopez-Gimenez, F.J.; Castro, M.D.L.; Dorado, G.; Dorado, M.P. The ideal vegetable oil-based biodiesel composition: A review of social, economical and technical implications. *Energy Fuel* **2009**, *23*, 2325–2341. [CrossRef]
30. Tangsriwong, K.; Lapchit, P.; Kittijungjit, T.; Klamrassamee, T.; Sukjai, Y.; Laoonual, Y. Modeling of chemical processes using commercial and open-source software: A comparison between Aspen Plus and DWSIM. *IOP Conf. Ser. Earth Environ. Sci.* **2020**, *463*, 012057.
31. Medeiros, D. DWSIM—Open Source Process Simulator. Available online: <http://sourceforge.net/projects/dwsim> (accessed on 15 May 2023).
32. Almeida, L.A.; Vilas Bôas, R.N.; Mendes, M.F. Process simulation of biodiesel production from vegetable oil deodorization distillate using hydrotalcite-hydroxyapatite as catalyst. *Res. Soc. Dev.* **2021**, *10*, e15210615452. [CrossRef]
33. Da Cruz, D.M.B.; da Silva, C.M.C.B.; de Souza Menezes, J.D.; Magalhães, A.M.C.; de Faro, F.S. Optimization of biodiesel and glycerol production process from palm oil and soy by modeling in DWSIM software. *Braz. J. Dev.* **2021**, *7*, 77121–77145. [CrossRef]
34. Cortes-Peña, Y.; Kumar, D.; Singh, V.; Guest, J.S. BioSTEAM: A Fast and Flexible Platform for the Design, Simulation, and Techno-Economic Analysis of Biorefineries under Uncertainty. *ACS Sustain. Chem. Eng.* **2020**, *8*, 3302–3310. [CrossRef]
35. Hassan, M. A simulation of energy generation from Jatropha solid residues in a power plant in Jazan city, KSA. *Heliyon* **2022**, *8*, e09352. [CrossRef]
36. Parente, E.J.S., Jr.; de Oliveira, L.B.; Luna, F.M.T.; Cavalcante, C.L., Jr. Integrated production of biolubricants and biodiesel: Process simulation and technical–economic analysis. *Biomass Convers. Biorefin.* **2023**, *13*, 1–24. [CrossRef]
37. Canakci, M.; Sanli, H. Biodiesel production from various feedstocks and their effects on the fuel properties. *J. Ind. Microbiol. Biot.* **2008**, *35*, 431–441. [CrossRef] [PubMed]
38. ASTM D891; Standard Test Methods for Specific Gravity, Apparent, of Liquid Industrial Chemicals. Book of Standards, Volume: 06.04; ASTM International: West Conshohocken, PA, USA, 2018. [CrossRef]
39. ASTM D1293; Standard Test Methods for pH of Water. Book of Standards Volume: 11.01; ASTM International: West Conshohocken, PA, USA, 2018. [CrossRef]
40. ASTM D1125; Standard Test Methods for Electrical Conductivity and Resistivity of Water. Book of Standards Volume: 11.01; ASTM International: West Conshohocken, PA, USA, 2014. [CrossRef]

41. ISO 2098; Glycerols for Industrial Use—Determination of Ash—Gravimetric Method. International Organization for Standardization: Geneva, Switzerland, 1972.
42. AOCS EA 6-94; Determination of Crude Glycerin, Titrimetric Method, AOCS Official Method. American Oil Chemists' Society: Urbana, IL, USA, 2009.
43. Nanda, M.R.; Yuan, Z.; Qin, W.; Poirier, M.A.; Chunbao, X. Purification of crude glycerol using acidification: Effects of acid types and product characterization. *Austin J. Chem. Eng.* **2014**, *1*, 1004.
44. Ferreira, M.O.; Sousa, M.E.B.D.; Pereira, C.G. Purification of crude glycerine obtained from transesterification of cottonseed oil. *Int. J. Chem. React. Eng.* **2013**, *11*, 385–392. [[CrossRef](#)]
45. Hutchison, B.R.M.; Wallace, J.S. Influence of fuel volatility on particulate matter emissions from a production DISI engine. *Fuel* **2021**, *303*, 121206. [[CrossRef](#)]
46. Dobrowolski, A.; Miłuta, P.; Rymowicz, W.; Mirończuk, A.M. Efficient conversion of crude glycerol from various industrial wastes into single cell oil by yeast *Yarrowia lipolytica*. *Bioresour. Technol.* **2016**, *207*, 237–243. [[CrossRef](#)] [[PubMed](#)]
47. Escribà, M.; Eras, J.; Villorbina, G.; Balcells, M.; Blanch, C.; Barniol, N.; Canela, R. Use of Crude Glycerol from Biodiesel Producers and Fatty Materials to Prepare Allyl Esters. *Waste Biomass Valoriz.* **2011**, *2*, 285–290. [[CrossRef](#)]
48. Indran, V.P.; Saud, A.S.H.; Maniam, G.P.; Taufiq-Yap, Y.H.; Rahim, M.H.B. Viable Glycerol Carbonate Synthesis Through Direct Crude Glycerol Utilization from Biodiesel Industry. *Waste Biomass Valoriz.* **2017**, *8*, 1049–1059. [[CrossRef](#)]
49. Sittijunda, S.; Reungsang, A. Methane Production from the Co-digestion of Algal Biomass with Crude Glycerol by Anaerobic Mixed Cultures. *Waste Biomass Valoriz.* **2020**, *11*, 1873–1881. [[CrossRef](#)]

Disclaimer/Publisher's Note: The statements, opinions and data contained in all publications are solely those of the individual author(s) and contributor(s) and not of MDPI and/or the editor(s). MDPI and/or the editor(s) disclaim responsibility for any injury to people or property resulting from any ideas, methods, instructions or products referred to in the content.